Supporting Information

Molecular Dynamics Study on Elucidation of Polyamide Membrane Fouling by Nonionic Surfactants and Disaccharides

Yuki Kawabata,[a,b] Ralph Rolly Gonzales,[b] Keizo Nakagawa,[a,b] Takuji Shintani,[a,b] Hideto Matsuyama,[b,c] Yu Fujimura,[d] Takahiro Kawakatsu,[d] and Tomohisa Yoshioka [a,b]*

[a]Graduate School of Science, Technology and Innovation, Kobe University, 1-1 Rokkodai, Nada, Kobe 657-8501, Japan

[b]Research Center for Membrane and Film Technology, Kobe University, 1-1 Rokkodai, Nada, Kobe 657-8501, Japan

[c]Department of Chemical Science and Engineering, Kobe University, 1-1 Rokkodai, Nada, Kobe 657-8501, Japan

[d]Research and Development Division, Kurita Water Industries Ltd., 1-1, Kawada, Nogi, Shimotsuga, Tochigi 329-0105, Japan

*Corresponding author: Tomohisa Yoshioka; Email: tom@opal.kobe-u.ac.jp

Detail of COMPASS Ⅱ

Atomic charge

Figure S1 shows the charge of each atom of water molecule and PE5, Mal, and **Figure S2** shows the charge of each atom of PA membrane.
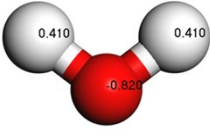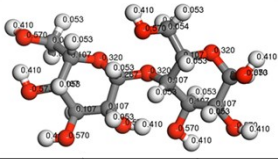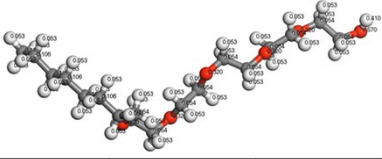

H₂O			Maltose			PE5		
Total charge =0			Total charge =0			Total charge =0		
Atom	Charge	Quantity	Atom	Charge	Quantity	Atom	Charge	Quantity
H	0.410	2	C	0.107	8	H	0.053	37
O	-0.820	1	O	-0.32	3	C	-0.159	1
			O	-0.57	8	C	-0.106	6
			H	0.053	14	C	0.054	11
			C	0.054	2	O	-0.32	5
			H	0.41	8	O	-0.57	1
			C	0.267	2	H	0.41	1

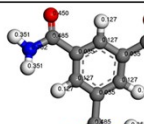**Figure S1.** Atomic charges of water molecules and PE5 and Mal.
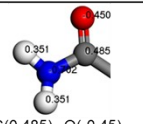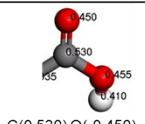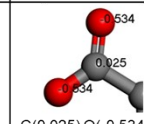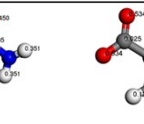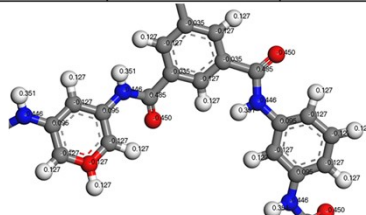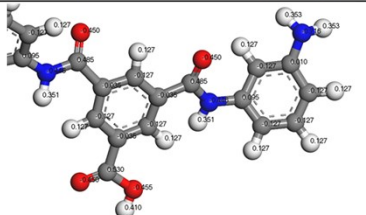
Polyamide											
P-CN		P-C0		P-C4		P-C7		P-C11		P-C22	
Total charge = 0		Total charge = 0		Total charge ≒ - 2.002		Total charge ≒ -4.004		Total charge ≒ -6.006		Total charge ≒ -12.012	
Atom Charge	N_{atom}	Atom Charge	N_{atom}	Atom Charge	N_{atom}	Atom Charge	N_{atom}	Atom Charge	N_{atom}	Atom Charge	N_{atom}
N -0.716	6	N -0.716	6	N -0.716	6	N -0.716	6	N -0.716	6	N -0.716	6
N -0.702	54	O -0.455	54	O -0.534	4	O -0.534	8	O -0.534	12	O -0.534	24
O -0.45	180	O -0.45	180	O -0.455	52	O -0.455	50	O -0.455	48	O -0.455	42
N -0.446	126	N -0.446	126	O -0.45	178	O -0.45	176	O -0.45	174	O -0.45	168
C -0.127	444	C -0.127	444	N -0.446	126	N -0.446	126	N -0.446	126	N -0.446	126
C -0.035	180	C -0.035	180	C -0.127	444	C -0.127	444	C -0.127	444	C -0.127	444
C 0.01	6	C 0.01	6	C -0.035	178	C -0.035	176	C -0.035	174	C -0.035	168
C 0.095	126	C 0.095	126	C 0.01	6	C 0.01	6	C 0.01	6	C 0.01	6
H 0.127	444	H 0.127	444	C 0.025	2	C 0.025	4	C 0.025	6	C 0.025	12
H 0.351	234	H 0.351	126	C 0.042	2	C 0.042	4	C 0.042	6	C 0.042	12
H 0.353	12	H 0.353	12	C 0.095	126	C 0.095	126	C 0.095	126	C 0.095	126
C 0.485	180	H 0.41	54	H 0.127	444	H 0.127	444	H 0.127	444	H 0.127	444
		C 0.485	126	H 0.351	126	H 0.351	126	H 0.351	126	H 0.351	126
		C 0.53	54	H 0.353	12	H 0.353	12	H 0.353	12	H 0.353	12
				H 0.41	52	H 0.41	50	H 0.41	48	H 0.41	42
				C 0.485	126	C 0.485	126	C 0.485	126	C 0.485	126
				C 0.53	52	C 0.53	50	C 0.53	48	C 0.53	42

Polar group of polyamide			
CONH₂	COOH	COO-	Benzene ring
C(0.485) O(-0.45) N(-0.702) H(0.351)	C(0.530) O(-0.450) O(-0.455) H(0.410)	C(0.025) O(-0.534) O(-0.534)	

Figure S2. Atomic charges of polyamide membrane.

Simulation method

PA membrane units were modeled using 30 MPDs and 33 TMCs. The degree of cross-linkage (*DC*) was calculated using eqS2.

$$DC = \frac{100 \times N_N}{N_N + N_{COOH}}$$

(S2)

In eq S2, N_N indicates the number of nitrogen atoms in the PA molecule, and N_{COOH} indicates the number of -COOH groups. This model used the PA membrane with a *DC* of 71%, which approximates the degree of cross-linking (68.8%) of actual PA. [1,2]

The PA membrane unit was modeled using three single-layer PA membranes with 71% of diagonal cross-linking. After structural optimization, MD calculation was performed using an NVT ensemble at 298 K for 0.50 ns. Furthermore, 65 water molecules were added to the cell at a saturation density of 1.37 g/cm^3, which was intended to approximate the density of the actual experimental hydrated PA membrane (**Figure S3**).[3]
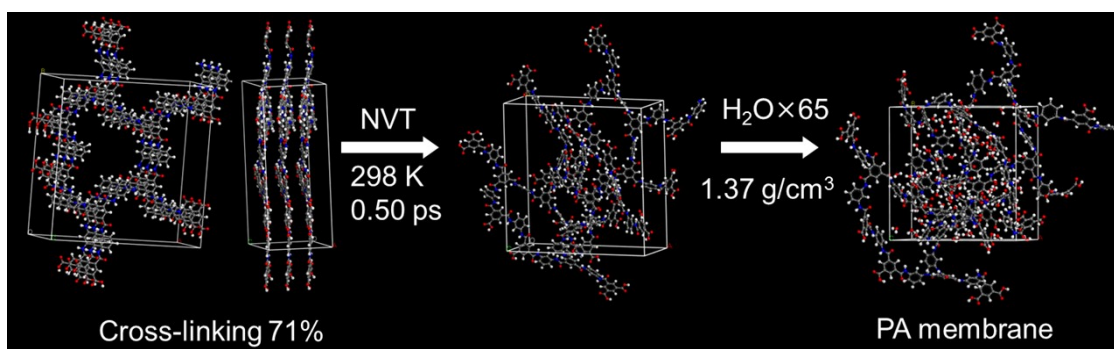

Figure S3. Model of the PA membrane unit.

Water-PA system

Mean square displacement

Mean square displacement (MSD) was analyzed for O atoms of all water molecules in the system. The diffusion coefficient of water molecules in the water-PA system and bulk water system was calculated using the MSD and Einstein equations. It was calculated from a slope that ranged from 1.0- 3.0 ns of MSD, as shown in **Figure S4**.
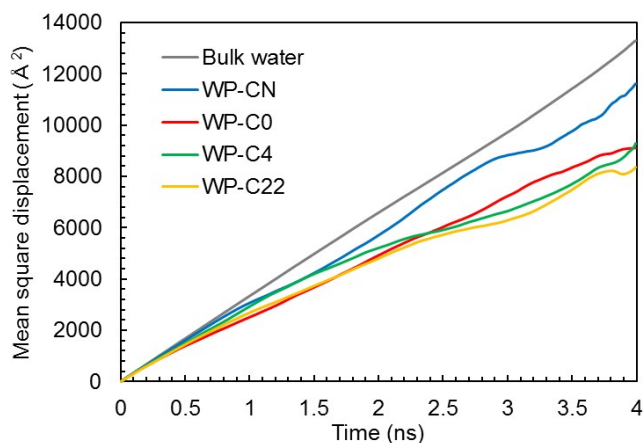
Figure S4. Mean square displacement of water in the Water-PA system.

Density distribution of water molecules

Figure S5 shows the density distribution of water molecules in the water-PA systems with different states of functional groups. The zero Å location on the horizontal axis indicates the PA-Water interface, which occurred at -30 to zero Å for the aqueous phase region and at zero to 25 Å for the PA membrane region. The density distribution, $\rho(z)$, was calculated from the number of water molecules in the aqueous phase divided by 0.5 Å in the z-axis direction, as shown in eq S**3**:

$$\rho(z) = \frac{MN(z)}{N_A \Delta V}$$

(S3)

In eq S3, M is the molecular weight of the water molecule, $N(z)$ is the number of water molecules in a volume of ΔV = 28.68 Å × 28.68 Å × 0.5 Å in the x, y, and z axis directions at the z location, and N_A is Avogadro's number.

The water molecular density was nearly constant at around 1.0 g/cm^3 and when z = -30 to -10 Å corresponding to the interfacial water phase. Approaching the PA surface, the density was decreased due to the increase in occupied volume by the PA molecules for all models. There was no significant difference in the density distributions of WP-CN, WP-C0, and WP-C4, which indicated that the density of the water molecules in the PA membrane were consistently about 0.1 g/cm^3. This trend agrees with previously reported results found in the literature.[4] On the other hand, the water molecular density distribution of WP-C22 differed the most from the others. The water density in WP-C22 had a small peak around the z = 5 Å region on the aqueous phase side of the water-PA interface. The molecular density of water was higher in the 10Å region of the PA membrane surface than it was in the same area of the other systems. This indicated a hydrophilization of the PA membrane surface due to the dissociation of the carboxyl group. Hydrophilization due to dissociation of PA membrane and changes in membrane characteristics due to amination have also been reported experimentally.[5,6,7]
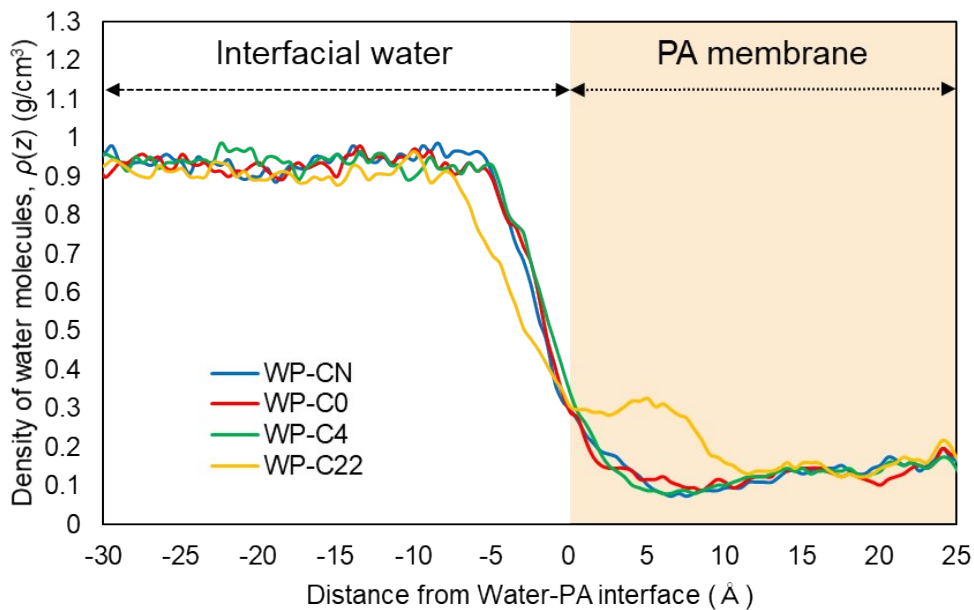
Figure S5. Density distribution of water molecules.

As a result of the characteristics of the Water-PA systems, the states of water molecules on the surfaces of the PA membranes caused by the changes in the carboxyl groups are summarized in **Figure S6**. Based on the analysis of the orientation vector and RDF of water molecules on the PA membrane surfaces, we speculated that in WP-CN, where all the carboxyl groups terminated with -CONH$_2$, the water molecules were not constrained by the functional groups and had a low orientation with the membrane surface. In WP-C0, we presumed that water molecules were localized around the carboxyl groups with oxygen atoms directed toward the carboxyl groups, and the orientation was low near the surface. In WP-C4, the water molecules were slightly more orientated to the surface than in WP-C0. As **Figure S6** shows, the second hydration layer in the PA-water interface on WP-C22 facilitated the highest order of water molecular orientation among all Water-PA systems.
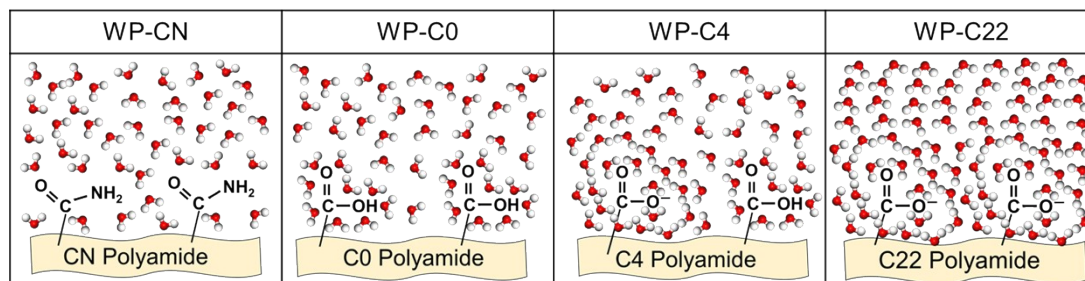

Figure S6. State and orientation of water molecules in Water-PA systems with different functional groups in the PA.

Foulant-PA system

The behaviors of PE5 and Mal were analyzed via the average distance of PE5 or Mal from the PA-water interface and the energy of interaction between PE5 or Mal and the PA membrane.

In order to examine the adsorption of foulants (PE5, Mal), the average distance between these molecules and the PA surface was analyzed for a simulation period of from 1 to 4 ns. **Figure S7(a)** shows the distances between the Water-PA interface and the terminal carbon and oxygen of PE5. **Figure S7(b)** shows the distance between the Water-PA interface and the terminal oxygen atom of Mal in the Water-PA interface. These results showed that both PE5 and Mal were adsorbed onto the PA membrane. In PP-C0, however, PE5 was deposited more deeply inside the PA membrane than Mal in MP-C0. It is apparent that the alkyl group adsorbs onto the PA membrane in the PP-C0 system, and the hydroxyl group of PE5 adsorbs to the PA membrane in the PP-C11 and PP-C22 systems. The PA membrane with higher hydrophobicity adsorbed the hydrophobic group of PE5, while the more hydrophilic PA membrane adsorbed the hydrophilic group of PE5. These results showed that amphipathic nonionic surfactants such as PE5 behave differently at the PA-water interface, which depends on the dissociation degree of the carboxyl groups of PA. MP-C0, MP-C4, and MP-C7 in **Figure S7(b)** show that Mal became stable on the PA surface. This is thought to be due to the stability of a disaccharide with water molecules because of the presence of hydroxyl groups in the Mal molecule.
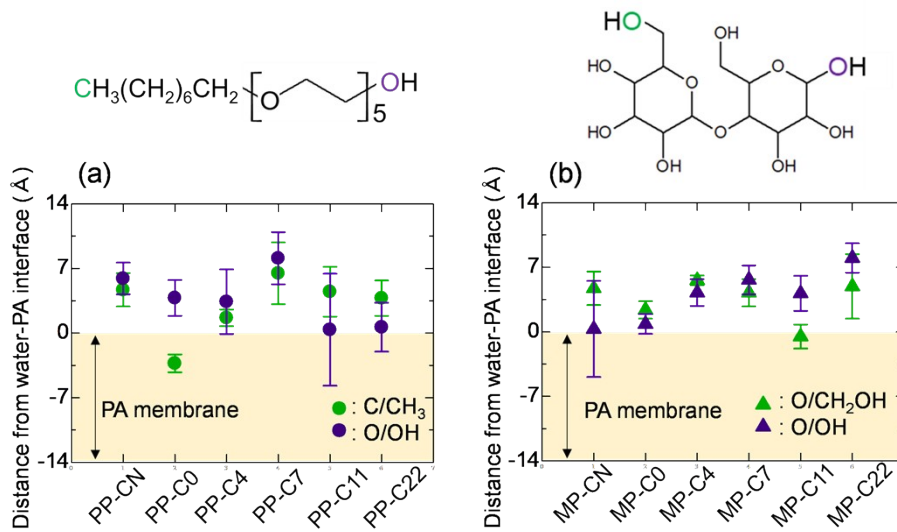
Figure S7. Average distances of (a) PE5 and (b) Mal from the Water-PA interface.

Figure S8 shows the accumulated localized number of water molecules around the functional group. It was shown that the number of water molecules around the functional group was smaller in WP-CN than in WP-C0, WP-C4 and WP-C22. In this study, the coordination number was calculated using eq. S4 that is a same method reported in the previous papers[8],[9]. For the coordination numbers in **Figure 4** and **Figure S9**, the coordination numbers at r = 3 Å were used as the first hydration numbers shown in **Figure S8**, respectively. The coordination numbers at r = 3Å were 4 in WP-CN, 9 in WP-C0, 8 in WP-C4, and 10 in WP-C22, respectively.

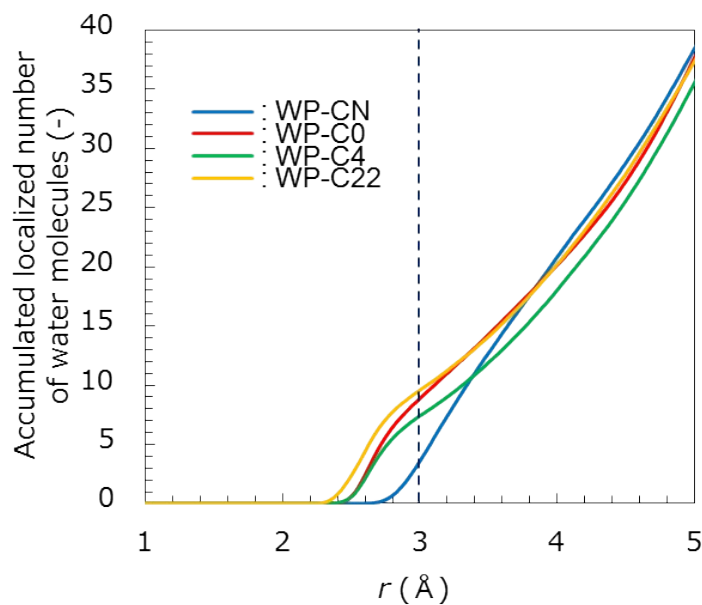$$n(r) = 4\pi r^2 \Delta r \rho g(r) \qquad (S4)$$

Figure S8. Accumulated localized number of water molecules around the functional group.

Schematic diagram of the PA membrane surface

Figure S9 shows a schematic diagram of the PA membrane surface, water structures and their effect on adsorption behavior of PE5 and Mal molecules. It should be noted that this figure is schematically illustrated for easy understanding of the phenomena in the vicinity of a PA membrane surface at the expense of accuracy.
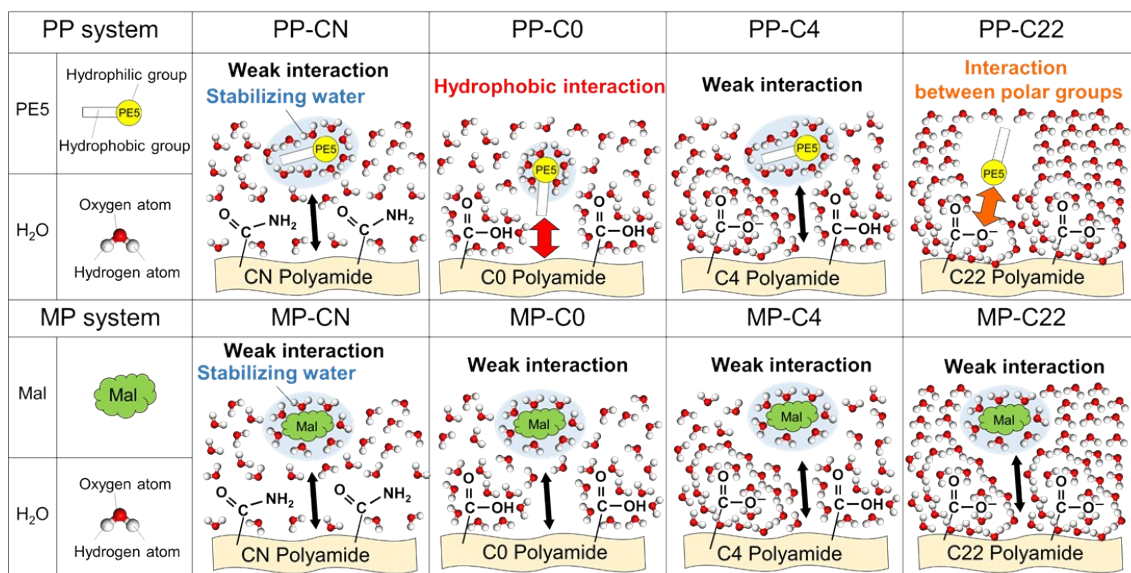

Figure S9. Schematic diagram of the surface of a PA membrane and its effect on the structure of water and on the adsorptions of both PE5 and Mal.

Water flux measurement apparatus (Experimental section)

Permeation experiments with nonionic surfactant aqueous solutions were also conducted for PA membranes under different pH conditions and for amine-modified PA membranes. The effect of pH, as measured by the dissociation amount of the carboxyl groups, and the effect of amine modification on the fouling behavior of nonionic surfactants showed good agreement with the above simulation results.

In experiments to support the simulation results, two factors affecting the water permeability of PA membranes were examined during the filtration of an aqueous solution of nonionic surfactants. One factor was the effect of the dissociation state of carboxyl groups under different pH conditions. The other factor was the effect of the amination of carboxyl groups. For the latter experiment, the residual carboxyl groups on a homemade PA membrane were modified with a secondary amine.

Membrane preparation

An ultrafiltration membrane, CF-30 (Nitto Denko Co.), made of polysulfone was used as a support membrane. Hydrochloric acid (HCl), *m*-phenylenediamine (MPD), sodium dodecyl sulfate (SDS), and 1,4-diaminobutane (BDA, **Figure S10**) were all from FUJIFILM Wako Pure Chemical Co. Isopropyl alcohol (IPA) was obtained from KISHIDA CHEMICAL Co., Ltd.; Polyoxyethylene octyl ether (PE5) and tetraethylene glycol monooctyl ether (TEG) were

obtained from Sigma-Aldrich Co., LLC. Water permeability measurements were performed using three commercially available membranes, ES-20 (Nitto Denko Co.), and two membranes were homemade: the first was a normal PA membrane (MPD-TMC) prepared by interfacial polymerization of MPD aqueous solution and TMC hexane solution;[10] and, the second was a modified PA membrane prepared by aminating the residual carboxyl group of the MPD-TMC membrane. The MPD aqueous solution was composed of 1 wt% MPD, 0.15 wt% SDS, and 5.0 wt% IPA, and the TMC hexane solution contained 0.1 wt% TMC and 0.05 wt% IPA. A linear aliphatic amine monomer, BDA, was used as a modifier for post-treatment of the MPD-TMC membrane to obtain an MPD-TMC-BDA version. A BDA aqueous solution containing 2.0 wt% BDA, 0.15 wt% SDS, and 5.0 wt% IPA was also prepared as an example of modification.

The support layer was washed with ultrapure water (Milli-Q) at 25 °C. Then, 40 mL of MPD aqueous solution was poured onto the support membrane. After 1 minute, the excess MPD aqueous solution was removed and replaced with 40 mL of TMC hexane solution, which was then removed 1 minute later. Any excess TMC hexane solution was also removed. To prepare an MPD-TMC-BDA membrane, 40 mL of the BDA aqueous solution was additionally poured onto the support membrane, and the excess was removed 1 minute later. The product was then dried at 110 °C for 2 minutes followed by drying at 25 °C for 16 hours. Finally, the membranes were washed with ethanol and immersed in water for storage in a cool dark place. In order to examine the effect that dissociated -COOH groups could exert on the water permeability of a PE5 aqueous solution, water flux was measured under different pH conditions. In the measurements, ES20 served as the PA membrane, and a 20 ppm PE5 aqueous solution was the nonionic surfactant.

Water permeation measurements

Water permeability measurements were conducted to investigate the effect of pH on the fouling of PA membranes by actual nonionic surfactant aqueous solutions. These were performed at a flow rate of 9.9 ml/min at 25 °C under an applied pressure of 1.0 MPa using the apparatus shown in **Figure S11**. The pH rates were 2.67 (isoelectric point of ES-20, **Figure S12**) and 6. The pH of the acidic aqueous solutions was controlled to 2.67 via the use of HCl. Water with the same pH, and without PE5, was fed every 30 min to investigate the recovery behavior of the water flux after fouling. Water permeability measurements were also carried out using ES-20, MPD-TMC and MPD-TMC-BDA membranes to study the effect that the functional groups of PA membranes exert on fouling behaviors. In this case, 50 ppm TEG aqueous solution (pH = 7) was used as the nonionic surfactant solution. The operating pressure was adjusted so that the pure water permeation flux was 1.1 m/d at 25 °C (**Figure S11**).

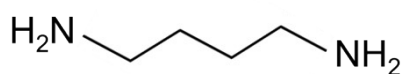The structural formula of 1.4-diaminobutane is shown in **Figure S10**.

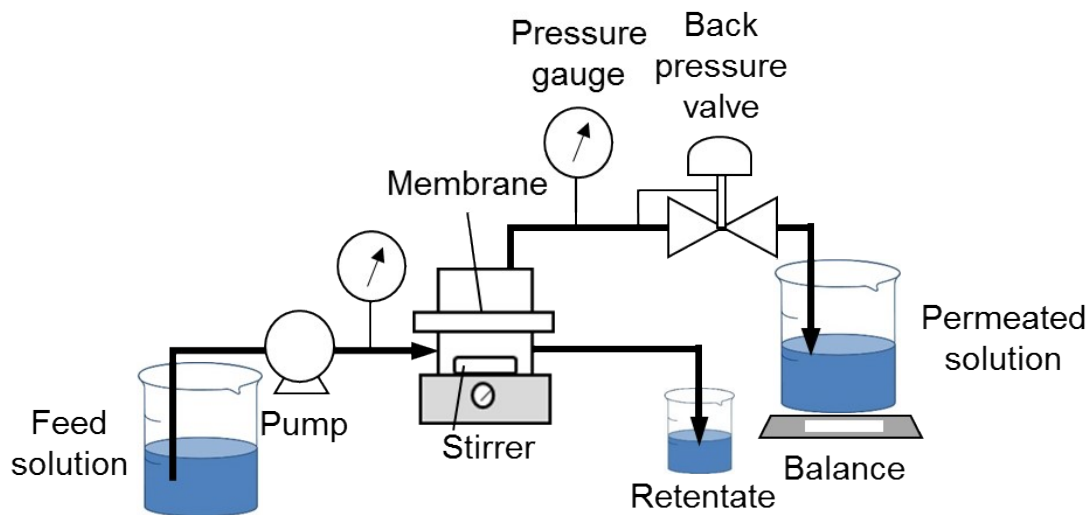**Figure S10**. Molecular formula of 1,4-Diaminobutane.

Figure S11. Schematic image of the water flux measurement apparatus.

Zeta potential of ES-20

Anton Paar GmbH's SurPASS^{TM}3 was used for the zeta potential measurement. One mmol / L KCl was used as the aqueous electrolyte. From **Figure S12** shows an isoelectric point of ES-20 at pH = 2.67.
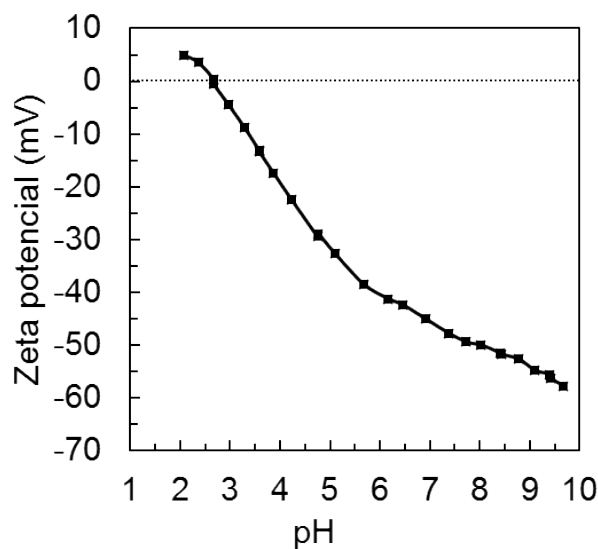

Figure S12. Zeta potential of ES-20.

Experimental fouling behavior

The changes in water permeation flux, J_w, for fouling experiments were compared by normalizing the initial water flux, J_{w0}, in each experiment. **Figure S13** shows the effect of different pH conditions on the normalized water flux of

the ES-20 membrane in the PE5 solution. The observed water flux decreased along with time for both pH conditions, and the decrease in water flux was greater under an isoelectric point of pH = 2.67. Then, the water flux was gradually recovered when feeding water without PE5 both at pH = 2.67 and pH = 6. However, the recovery ratio under a PE5 condition of 0 ppm was smaller when pH = 2.67. This could be due to the stronger fouling of PE5 under certain levels of pH, which also correlated with the behavior of PE5 during hydrophobic interactions in the PP-C0 system, as shown in **Figure S9**. The decrease in water flux at pH = 6 was smaller than that under the isoelectric point when the pH = 2.67. According to past papers, a carboxyl group dissociation ratio of 4% corresponds to pH values ranging from 4.8 to 6.5.[5] We can reasonably assume that the surface structure of a PA membrane in a system with a pH = 6 would be similar to that of the PP-C4 simulation model. On the other hand, the isoelectric point of PA membranes corresponds to that of the PP-C0 simulation model. In simulation results, the hydrophobic interaction in the PP-C0 was reduced by the slight hydrophilization of the PA membrane in PP-C4, which could prevent fouling by PE5. This agrees well with the experimental results showing that a decrease in water flux was reduced at pH = 6. These results suggest that hydrophilization of a PA membrane caused by the dissociation of a small number of carboxyl groups would be effective in suppressing the fouling of PA membranes by PE5.
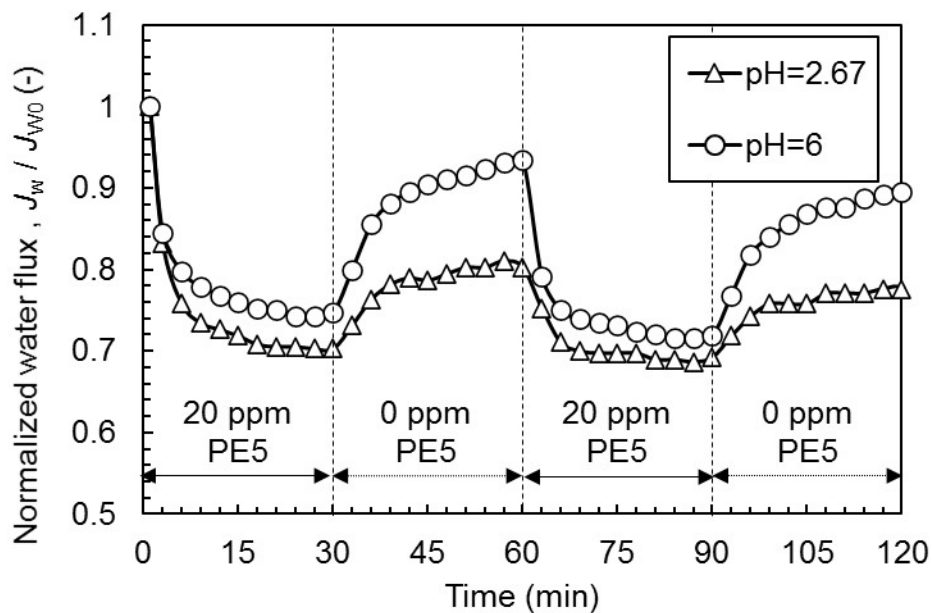

Figure S13. Time course of water flux through an ES-20 membrane for a 20 ppm PE5 aqueous solution under different pH conditions.

Figure S14 shows the time course of the water flux for a TEG aqueous solution while permeating a PA membrane and through an aminated PA membrane at pH = 7. A decrease in water permeability was observed for all membranes over time. Unlike the sharp decreases in the water flux for the first two hours of operation using ES-20

10

and MPD-TMC membranes, the decrease in water flux for a MPD-TMC-BDA membrane was much lower. The reduction rate for the initial water flux was about 40% for the commercially available RO membrane ES20 and the homemade MPD-TMC membrane, while it was about 20% for the MPD-TMC-BDA membrane. This suggests that the BDA-modified PA membrane significantly reduced fouling compared with the unmodified PA membranes. In the MD simulation, this tendency was qualitatively consistent with the results of reduced hydrophobic interactions in the amino group-modified PP-CN model. Based on the simulation results shown in **Figure S9**, we predicted that free water that is not localized near the functional groups of a PA membrane could reduce the adsorption of amphipathic surfactant molecules on the membrane surface. Experimental results also revealed the effectiveness of modifying dissociative carboxyl groups with an amino group. The experimental water flux measurements showed the same tendency as the simulation results, which validates our simulation data.
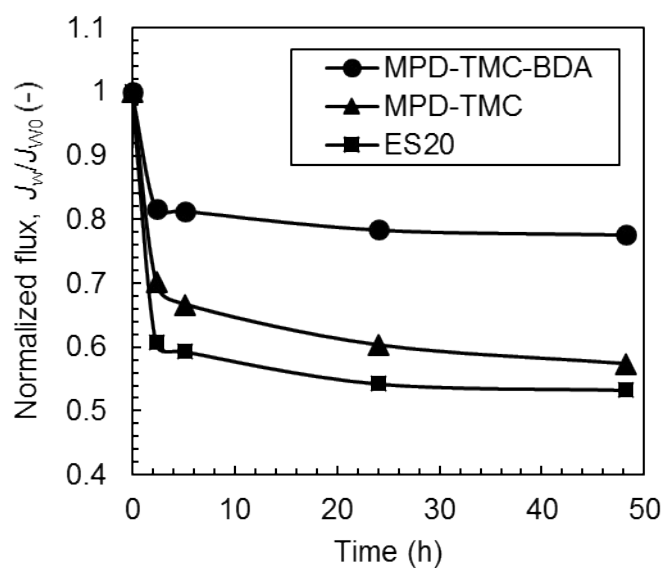

Figure S14. Time course of water flux for three different membranes (pH = 7).

11

References

1. O. Coronell, B. J. Mariñas and D. G. Cahill, *Environmental Science & Technology*, 2011, **45**, 4513-4520.

2. T. Yoshioka, K. Kotaka, K. Nakagawa, T. Shintani, H.-C. Wu, H. Matsuyama, Y. Fujimura and T. Kawakatsu, *Membranes*, 2018, **8**.

3. B. Mi, D. G. Cahill and B. J. Mariñas, *Journal of Membrane Science*, 2007, **291**, 77-85.

4. Z. E. Hughes and J. D. Gale, *Journal of Materials Chemistry*, 2012, **22**, 175-184.

5. D. Chen, J. R. Werber, X. Zhao and M. Elimelech, *Journal of Membrane Science*, 2017, **534**, 100-108.

6. D. Chen, Q. Chen, T. Liu, J. Kang, R. Xu, Y. Cao and M. Xiang, *RSC Advances*, 2019, **9**, 20149-20160.

7. Y.-N. Kwon, S. Hong, H. Choi and T. Tak, *Journal of Membrane Science*, 2012, **415-416**, 192-198.

8. Y. Han, L. Wu, T. Jiao and Q. Gao, *Langmuir*, 2020, **36**, 8922-8928.

9. H.-C. Wu, T. Yoshioka, K. Nakagawa, T. Shintani, T. Tsuru, D. Saeki, Y.-R. Chen, K.-L. Tung and H. Matsuyama, *Desalination*, 2017, **424**, 85-94.

10. W. J. Lau, S. Gray, T. Matsuura, D. Emadzadeh, J. Paul Chen and A. F. Ismail, *Water Research*, 2015, **80**, 306-324.